

ICSV14
Cairns • Australia
9-12 July, 2007



IDENTIFICATION OF MACHINE TOOL CHATTER FOR MILLING OPERATIONS WITH RUNOUT

Tamas Inspirger¹, Brian P. Mann², Tobias Surmann³ and Gabor Stepan¹

¹Department of Applied Mechanics, Budapest University of Technology and Economics
1111 Budapest, Hungary

²Department of Mechanical and Aerospace Engineering, University of Missouri-Columbia, Columbia,
MO 65211, USA

³Department of Machining Technology, University of Dortmund, 44369 Dortmund, Germany
inspi@mm.bme.hu

Abstract

Detection of undesired machine tool vibrations during milling operations is an important task for manufacturing engineers. Monitoring of frequency spectra is an efficient tool of chatter detection since these spectra usually have a clear, systematic structure. However, for some special cases, stability of the cutting process cannot be assessed based purely on the frequency spectra due to the disturbing effect of the runout of the tool. In this paper, it is shown that the stability of these cases can be assessed by the analysis of the vibration signal instead of the frequency spectra. Theoretical results are confirmed by experimental cutting tests.

1. INTRODUCTION

Machine tool chatter is still a problem for the machining community. These violent vibrations of the machine tool are problematic since they result in a poor surface finish, cause large-amplitude acoustic emissions, and can sometimes lead to tool failure. Therefore, it is highly important to detect the onset of these vibrations.

An efficient tool for identifying machine tool chatter is the monitoring of the vibration frequencies during machining. For ideal milling operations, vibration frequencies have a well defined, special structure, and the identification of stable and unstable machining cases is clear and trivial [1]. However, in practice, several other effects arise that influence and sometimes destroy this nice structure. One of them is the runout that is the state of the milling cutter with rotational axis differing from the geometric one. Runout causes the chip load to be distributed unevenly among the cutting teeth and shifts the frequency content of the cutting force signal away from the tooth passing frequency towards the spindle rotational frequency [2-5]. In this case, the distinction between stable and unstable cuts is not always possible based purely on the frequency spectrum [6]. For instance, in the case of a tool with even number of cutting teeth, the period doubling (flip) chatter frequencies coincides with the harmonics of the tool rotational frequencies that are caused by the runout, thus, these period doubling cases cannot be distinguished from stable machining (see, e.g., [7]). In this paper, the analysis of the vibration signal is proposed in addition to frequency spectra monitoring in order to assess the stability of the cutting process for these problematical cases.

2. MECHANICAL MODELL

The mechanical model of the milling operation with a compliant tool can be seen in Figure 1. The corresponding equation of motion reads

$$\mathbf{M}\ddot{\mathbf{x}}(t) + \mathbf{C}\dot{\mathbf{x}}(t) + \mathbf{K}\mathbf{x}(t) = a_p \mathbf{H}(t)(\mathbf{x}(t) - \mathbf{x}(t - \tau)). \quad (1)$$

The vector $\mathbf{x}(t)$ contains the displacement of the tool tip in the x and y directions. The matrices \mathbf{M} , \mathbf{C} and \mathbf{K} are the modal mass, damping and stiffness matrices, and a_p is the axial depth of cut. The time delay is equal to the tooth passing period: $\tau = \Omega/(N60)$, where Ω is the spindle speed in rpm and N is the number of teeth of the miller. The elements of the directional force coefficient matrix $\mathbf{H}(t)$ are

$$H_{xx}(t) = \sum_{j=1}^N \rho_j g_j(t) (K_t c_j(t) + K_n s_j(t)) s_j(t), \quad (2)$$

$$H_{xy}(t) = \sum_{j=1}^N \rho_j g_j(t) (K_t c_j(t) + K_n s_j(t)) c_j(t) \quad (3)$$

$$H_{yx}(t) = \sum_{j=1}^N \rho_j g_j(t) (-K_t s_j(t) + K_n c_j(t)) s_j(t) \quad (4)$$

$$H_{yy}(t) = \sum_{j=1}^N \rho_j g_j(t) (-K_t s_j(t) + K_n c_j(t)) c_j(t) \quad (5)$$

where K_t and K_n are the tangential and normal cutting coefficients with $c_j(t) = \cos(\varphi_j(t))$ and $s_j(t) = \sin(\varphi_j(t))$. The angular position $\varphi_j(t)$ of the j^{th} tooth is determined by the spindle speed Ω in the form $\varphi_j(t) = 2\pi\Omega t/60 + 2\pi(j-1)/N$. The function $g_j(t)$ defines if the j^{th} tooth is cutting or not

$$g_j(t) = \begin{cases} 1 & \text{if } \varphi_e < \varphi_j(t) < \varphi_a \\ 0 & \text{otherwise} \end{cases} \quad (6)$$

where φ_e and φ_a are the entry and exit angles of the cut.

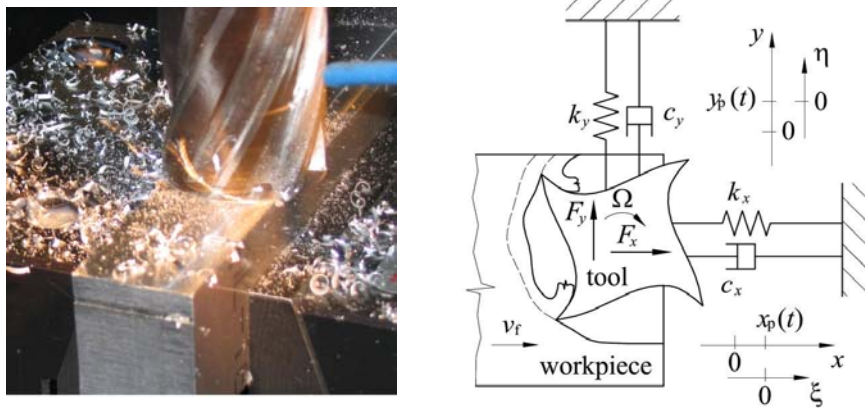


Figure 1. Milling operation and its mechanical model

The runout for each tooth is modelled by a single factor ρ_j . If there is no runout (i.e., $\rho_j = 1$, $j = 1, 2, \dots, N$), then matrix $\mathbf{H}(t)$ is periodic with the tooth passing period τ . In this case, the principal period of the system is equal to the time delay. This case corresponds to the conventional models of the milling process (see, e.g., [1, 8-10]).

In practical milling processes, runout cannot be avoided, i.e., $\rho_j \neq 1$, $j = 1, 2, \dots, N$. In this case, matrix $\mathbf{H}(t)$ is periodic with the tool rotation period $T = 60/\Omega = N\tau$. Usually, the discrepancies between the location of the teeth and between the cutting forces acting on them are small. This explains that a τ -periodic cutting force variation assumption is usually a good approximation, in spite of the fact that it is actually T -periodic. Figure 2 shows the variation of the cutting force acting on the tool during machining with a two fluted miller. It can clearly be seen that the teeth experience different loads. The accompanied Power Spectral Density (PSD) diagram shows the additional frequency peaks at the multiples of the tool rotation frequency ($1/T$, $3/T$, etc.).

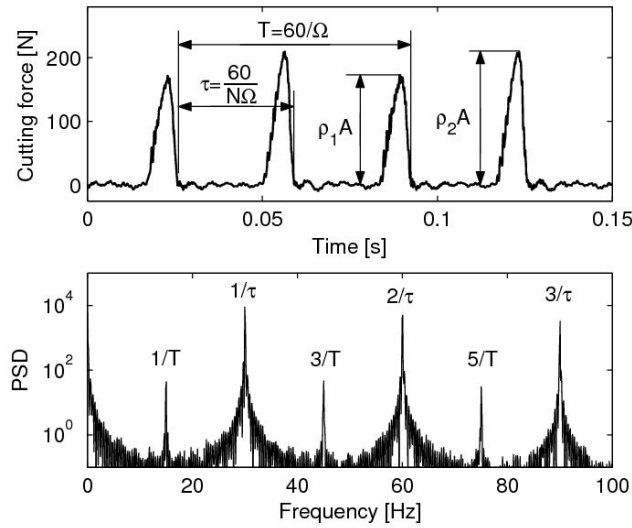


Figure 2. Cutting force and the corresponding PSD

3. STABILITY AND CHATTER FREQUENCIES

The vibrations of the tool can be decomposed into two parts as follows (see, e.g., [1] or [10])

$$\mathbf{x}(t) = \mathbf{x}_p(t) + \boldsymbol{\xi}(t), \quad (7)$$

where \mathbf{x}_p is the T -periodic component excited by the T -periodic cutting force, and $\boldsymbol{\xi}$ is the chatter component.

For a stable operation, the chatter component is zero ($\boldsymbol{\xi}(t) \equiv 0$), and the tool motion is described by the forced component \mathbf{x}_p only. Since the forcing is usually non-harmonic, the corresponding frequency spectra contains peaks at the multiples of the tool rotation frequency

$$f_{\text{TR}} = \frac{k}{T} = \frac{k\Omega}{60}, \quad k = 1, 2, \dots \quad (8)$$

Stability of the milling process can be estimated theoretically via the analysis of the variational system around the periodic motion \mathbf{x}_p . According to the Floquet theory of delayed differential equations [11], an infinite dimensional operator (monodromy operator) can be associated to the system. The eigenvalues of this operator, also called as characteristic multipliers or Floquet multipliers, describe the stability of the system. If all the characteristic multipliers are in modulus less than 1, then the system is asymptotically stable. Since the system has infinitely many characteristic multipliers, such stability calculations cannot be done in closed forms, but numerical approximations can be applied. Here, two methods are used, the semi-discretization method [12], and the time finite element method [9]. The basic point of both methods is that they provide a finite dimensional matrix approximation of the monodromy operator and the eigenvalues of this matrix can be determined numerically.

Let us denote the critical (maximal in modulus) characteristic multiplier by μ_1 . The corresponding characteristic root (also called characteristic exponent) is $\lambda_1 = \ln \mu_1 / T$. Clearly, the system is just on the stability limit, if $\text{Re } \lambda_1 = 0$, that is if $\lambda_1 = \pm i\omega$. According to the Floquet theory of periodic systems, the chatter component can be written as

$$\xi(t) = \mathbf{p}(t)e^{\lambda_1 t} + \bar{\mathbf{p}}(t)e^{\bar{\lambda}_1 t}, \quad (9)$$

where $\mathbf{p}(t) = \mathbf{p}(t+T)$ is a T -periodic function, and bar denotes complex conjugation. Fourier expansion of this periodic function with the substitution of $\lambda_1 = i\omega$ gives

$$\mathbf{p}(t) = \sum_{k=-\infty}^{\infty} C_k e^{i \frac{k2\pi}{T} t}, \quad (10)$$

where C_k are complex coefficients. Thus, the chatter component can be written as

$$\xi(t) = \sum_{k=-\infty}^{\infty} \left(C_k e^{i \left(\omega + \frac{k2\pi}{T} \right) t} + \bar{C}_k e^{-i \left(\omega + \frac{k2\pi}{T} \right) t} \right). \quad (11)$$

The exponents in (11) give the frequency content of the chatter motion in [rad/s]. The corresponding chatter frequencies in Hz are

$$f_{\text{chatter}} = \pm \frac{\omega}{2\pi} + \frac{k}{T} = \pm \frac{\omega}{2\pi} + \frac{k\Omega}{60} \quad [\text{Hz}], \quad k = \dots, -1, 0, 1, \dots \quad (12)$$

Of course, only the positive frequencies have physical meaning. Here, we can distinguish among 3 different cases: 1) Quasi-periodic chatter; 2) Period 1 chatter; and 3) Period 2 chatter.

3.1 Quasi-periodic chatter

The critical characteristic multiplier is a complex pair $(\mu_1, \bar{\mu}_1)$ located on the unit circle: $|\mu_1| = 1$. This type of stability loss corresponds to the secondary Hopf or Neimark-Sacker bifurcation of periodic systems that is topologically equivalent to the Hopf bifurcation of autonomous systems. In this case, quasi-periodic vibrations arise during the loss of stability. The corresponding chatter frequencies are

$$f_{QP} = \pm \frac{\omega}{2\pi} + \frac{k}{T} = \pm \frac{\omega}{2\pi} + \frac{k\Omega}{60} \quad [\text{Hz}], \quad k = \dots, -1, 0, 1, \dots \quad (13)$$

3.2 Period 1 chatter

The critical characteristic multiplier is $\mu_1 = 1$. This case corresponds to the period one bifurcation of periodic systems that is topologically equivalent to the saddle-node bifurcation of autonomous systems. In this case, the chatter frequencies are equal to the multiples of the spindle rotation frequency:

$$f_{P1} = 0 + \frac{k}{T} = \frac{k\Omega}{60} \quad [\text{Hz}], \quad k = \dots, -1, 0, 1, \dots \quad (14)$$

Note, that in the literature [1, 9-10], this case is referred to as period 2 (flip) chatter, since if the effect of runout is neglected, then the system is τ -periodic. However, if the runout is incorporated into the model, as it is in the current analysis, then the system is not τ -periodic but T -periodic, and, in mathematical sense, this type of instability is a period 1 instability.

3.3 Period 2 chatter

The critical characteristic multiplier is $\mu_1 = -1$. This case corresponds to the period two (period doubling or flip) bifurcation of periodic systems, and there is no topologically equivalent type of bifurcation for autonomous systems. In this case, the chatter frequencies are equal to the multiples plus a half of the spindle rotation frequency:

$$f_{P2} = \frac{1}{2T} + \frac{k}{T} = \frac{\Omega}{120} + \frac{k\Omega}{60} \quad [\text{Hz}], \quad k = \dots, -1, 0, 1, \dots \quad (15)$$

Note, again that this case is not the same as the period 2 instabilities in the literature [1, 9-10], since system (1) is in fact T -periodic due to the runout.

4. EXPERIMENTAL RESULTS

Cutting tests were performed on a 5-axis linear motor Ingersol machining center with a Fischer 40,000 rpm, 40 kW spindle. A 12.75 mm diameter, 106 mm overhang, carbide end mill was used during all stability tests. The modal parameters of the compliant tool are

$$\mathbf{M} = \begin{pmatrix} 0.044 & 0 \\ 0 & 0.048 \end{pmatrix} [\text{kg}]; \quad \mathbf{C} = \begin{pmatrix} 4.27 & 0 \\ 0 & 4.36 \end{pmatrix} \begin{bmatrix} \frac{\text{Ns}}{\text{m}} \\ \frac{\text{Ns}}{\text{m}} \end{bmatrix}; \quad \mathbf{K} = \begin{pmatrix} 9.14\text{e}5 & 0 \\ 0 & 1\text{e}6 \end{pmatrix} \begin{bmatrix} \frac{\text{N}}{\text{m}} \\ \frac{\text{N}}{\text{m}} \end{bmatrix}.$$

Cutting coefficients in the tangential and normal directions were determined during separate cutting tests on a Kistler Model 9255B rigid dynamometer. An aluminum 7050-T7451 block was down-milled at a 5% radial immersion and a feedrate of 0.127 mm/tooth. The estimated cutting coefficients for the given material were $K_r = 536 \text{ N/mm}^2$, $K_n = 1.87 \text{ N/mm}^2$. The spindle speed Ω and depth of cut a_p were changed for each cutting test to determine the onset of unstable vibrations. The runout parameters were estimated based on the cutting forces acting on the different teeth (see Figure 2): $\rho_1 = 0.9$, $\rho_2 = 1.1$.

The top left panel of Figure 3 presents the stability chart in the plane of spindle speed and depth of cut. Thick lines denote theoretical stability boundaries. Stable and unstable cutting tests are denoted by circles and by crosses, respectively, and limit cases are denoted by + signs.

The bottom left panel shows the theoretically predicted frequency diagram computed from the critical characteristic multipliers. Dashed lines denote the multiples of the tool rotation frequency. Four different parameter points were investigated:

- point P: stable cutting,
- point Q: period 2 chatter,
- point R: quasi-periodic chatter,
- point S: period 1 chatter.

Multiples of the tool rotation frequency are denoted by a circle for all the four points P, Q, R and S, these forcing frequencies are always present in the system, even in the case of stable machining. In the period 2 case (point Q), chatter frequencies are denoted by diamonds. In the quasi-periodic case (point R), chatter frequencies are denoted by squares. In the period 1 case (point S), chatter frequencies are denoted by triangles. Black filled markers denote the frequencies caused by the runout of the tool (see [6]).

Right panels of Figure 3 present the power spectra corresponding to cutting tests at points P, Q, R and S. Circles, squares, diamonds and triangles denote the tool rotation frequencies, the quasi-periodic frequencies, the period 2 frequencies and period 1 frequencies, respectively. It can be seen that the structure of the PSD diagram is in good agreement with the theoretically predicted frequencies.

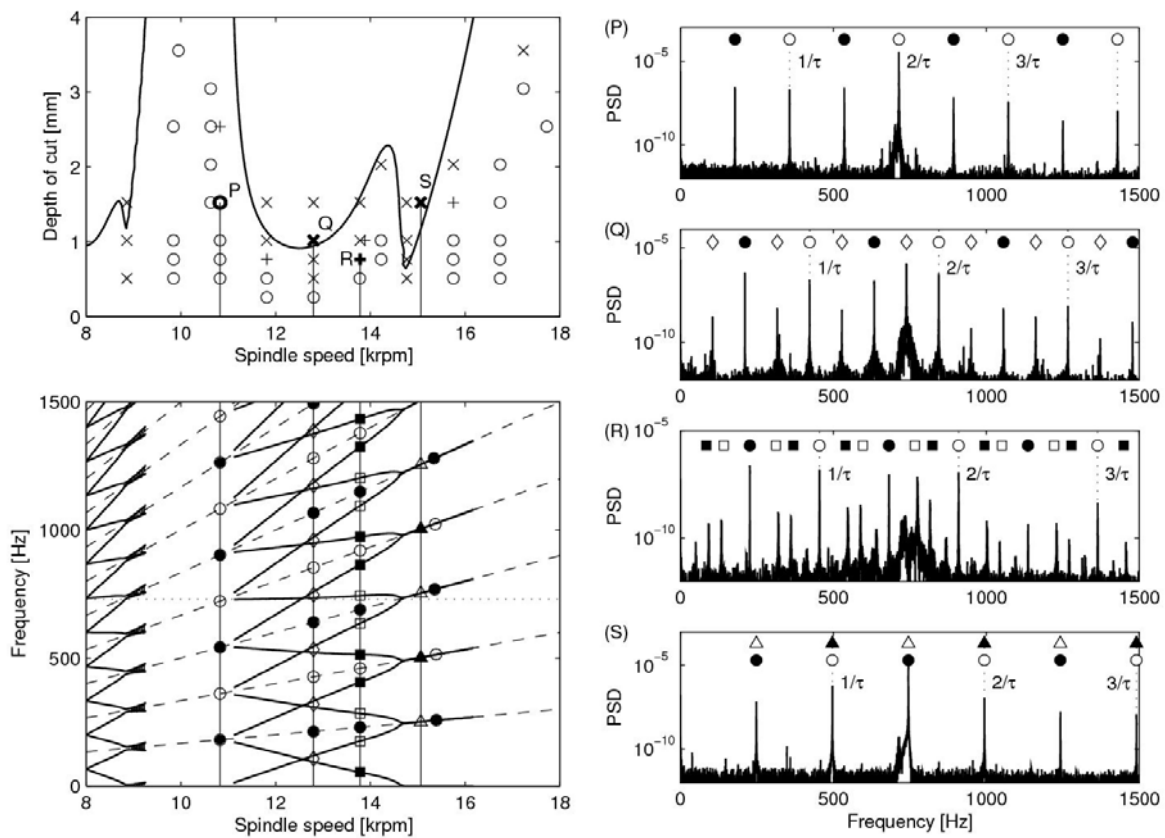


Figure 3. Stability chart and the corresponding vibrations frequencies

In the period 2 (point Q) and quasi-periodic (point R) cases, the presence of chatter can clearly be assessed based on frequency diagram. In the case of period 1 chatter, the chatter

frequencies coincides with the harmonics of the tool rotation frequency, resulting in a spectra that is qualitatively identical to the spectra of stable machining (see point P). Therefore, for period 1 case, the presence of chatter cannot be detected based on the frequency spectra. In order to overcome this problem, the vibration signals and Poincaré sections should be analysed directly, since they contain more information than the frequency spectra, e.g., the structure of the Poincaré sections clearly refers to the dynamic behaviour of the system (see, e.g., [10, 13, 14]).

Figure 4. shows the $1/\tau$ sampled time history of the vibrations and the corresponding Poincaré sections for both the stable (point P) and the period 1 (point S) cases. Note that the sampling is equal to the tooth passing period τ and not the tool rotation period T . Every second sampling is denoted by grey colour. This way, grey colour refers to position of the tool when tooth 1 is in the cut, while black colour refers to the position of the tool when tooth 2 is cutting. It can clearly be seen that in the stable case, the position of the tool is almost the same at each $1/\tau$ sampling. This small difference is caused by the different load acting on the different teeth, e.g., by the runout of the tool. In the period 1 case, this difference is more significant, one of the teeth (black) experiences essentially larger load than the other (grey). This is caused by the period 1 chatter (that is called period 2 in the literature [1, 9-10]). This difference is more obvious in the Poincaré sections. In the stable case, the grey and black points are very close to each other, while in the period 1 case, they clearly separate.

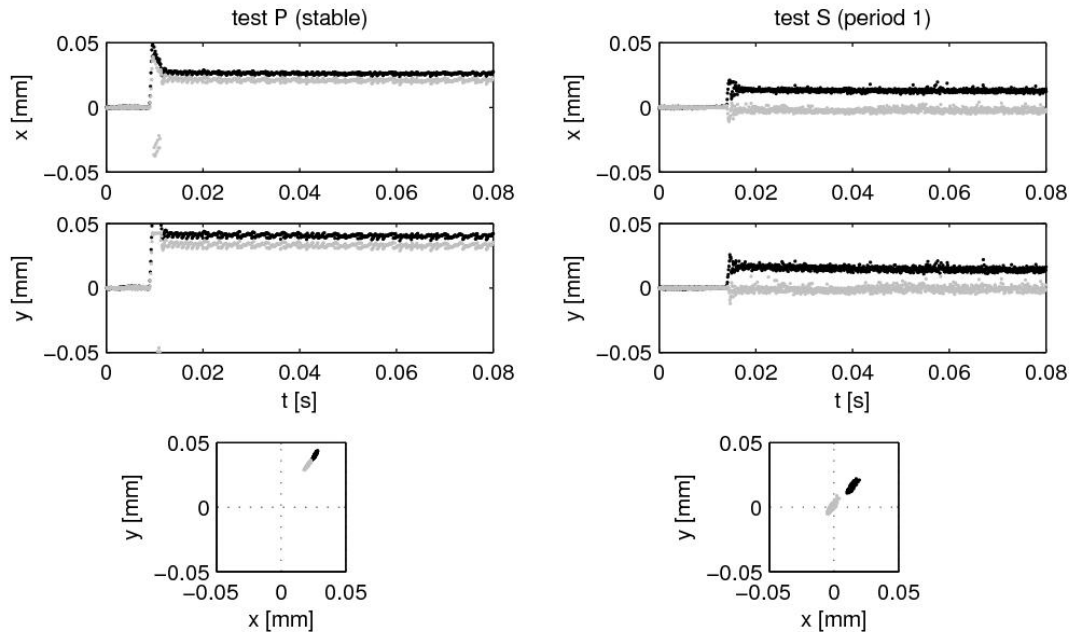


Figure 4. Vibration signal for the stable and the period 1 cases

6. CONCLUSIONS

Detection of machine tool chatter was investigated in the case of cutter runout based on frequency spectra and vibrations signals. It is known that the frequency spectra cannot be used to identify chatter in all cases due to the disturbance caused by the runout as it follows from the Floquet theory of time periodic delay differential equations. It was shown that for these cases, the vibration signal and the corresponding Poincaré sections can be used in order to assess the stability of the operation. The analysis was demonstrated for a milling operation with a two fluted tool and the results were verified experimentally.

ACKNOWLEDGEMENT

This research was supported in part by the János Bolyai Research Scholarship of the Hungarian Academy of Sciences, and by the Hungarian National Science Foundation under grant no. OTKA F047318 and OTKA T043368.

REFERENCES

- [1] T. Insperger, G. Stépán, P.V. Bayly, B.P. Mann, Multiple chatter frequencies in milling processes, *Journal of Sound and Vibration*, **262**(2), 333-345 (2003).
- [2] W.A. Kline, R.E. DeVor, The effect of runout on cutting geometry and forces in end milling, *International Journal of Machine Tool Design and Research*, **23**, 123–140 (1983).
- [3] H.Q. Zheng, X.P. Li, Y.S. Wong, A.Y.C. Nee, Theoretical modelling and simulation of cutting forces in face milling with cutter runout, *International Journal of Machine Tools & Manufacture*, **39**, 2003–2018 (1999).
- [4] X.P. Li, H.Z. Li, Theoretical modelling of cutting forces in helical end milling with cutter runout, *International Journal of Mechanical Sciences*, **46**, 1399–1414 (2004).
- [5] T.L., Schmitz, J. Couey, E. Marsh, N. Mauntler, D. Hughes, Runout effects in milling: Surface finish, surface location error, and stability, *International Journal of Machine Tools & Manufacture*, **47**, 841–851 (2007).
- [6] T. Insperger, B.P. Mann, B. Edes, G. Stépán, The effect of runout on the chatter frequencies of milling processes, *9th CIRP International Workshop on Modeling of Machining Operations*, Bled, Slovenia, 2006, paper no. 033 (CD-ROM).
- [7] M. Zatarain, J. Muñoa, G. Peigné, T. Insperger, Analysis of the influence of mill helix angle on chatter stability, *Annals of the CIRP*, **55**(1), 365-368 (2006).
- [8] Y. Altintas, E. Budak, Analytical prediction of stability lobes in milling, *Annals of the CIRP*, **44**(1), 357-362 (1995).
- [9] B.P. Mann, K.A. Young, T.L. Schmitz, D.N. Dilley, Simultaneous stability and surface location error predictions in milling, *Journal of Manufacturing Science and Engineering*, **127**(3), 446-453 (2005).
- [10] J. Gradišek, M. Kalveram, T. Insperger, K. Weinert, G. Stépán, E. Govekar, I. Grabec, On stability prediction for milling, *International Journal of Machine Tools and Manufacture*, **45**(7-8), 769-781 (2005).
- [11] M. Farkas, *Periodic Motions*, Springer-Verlag, New York, 1994.
- [12] T. Insperger, G. Stépán, Updated semi-discretization method for periodic delay-differential equations with discrete delay, *International Journal of Numerical Methods in Engineering*, **61**(1), 117-141 (2004).
- [13] T. Surmann, D. Enk, Simulation of milling tool vibration trajectories along changing engagement conditions, *International Journal of Machine Tools & Manufacture*, in press (2007).
- [14] G. Stépán, R. Szalai, B.P. Mann, P.V. Bayly, T. Insperger, J. Gradišek, E. Govekar, Nonlinear dynamics of high-speed milling – analyses, numerics and experiments, *Journal of Vibration and Acoustics*, **127**(2), 197-203 (2005).